IEEJ Journal of Industry Applications
Vol.8 No.2 pp.334–341 DOI: 10.1541/ieejjia.8.334

Paper

Advanced Deceleration Control Considering Driving Resistance by Predicting the Position of Pedestrians

Yusuke Nakamura[*a)] Student Member, Toshiyuki Murakami[*] Fellow

(Manuscript received May 2, 2018, revised Oct. 3, 2018)

This study aims to realize an automated deceleration system to avoid the collision of a vehicle with a pedestrian. The proposed system can predict a pedestrian's future position from the current position, and detect the collision probability. Furthermore, the controller employing model predictive control, which can compensate the driving resistance and the modeling error is also proposed. The effectiveness of the proposed method is verified through a simulation and experiment.

Keywords: Autonomous Emergency Braking System (AEBS), Model Predictive Control (MPC), Driving Force Observer (DFOB), Kalman filter

1. Introduction

The vehicle control technologies are rapidly developing as the advanced technology of information processing. For example, Antilock Brake System (ABS) that prevents the wheel lock during a sudden braking, Electronic Stability Control (ESC) that suppresses the tire slip under a slippery road conditions [(1)]. In addition, Direct Yaw moment Control (DYC) that controls the driving force of each wheel independently to stabilize the vehicle behavior, and the slip ratio control that maintains desired slip ratio by controlling driving force [(2)(3)]. With the development of such control technology, vehicles have become able to run more safely and stably than ever. The driving support system contributes greatly to the reduction of the number of traffic accidents, and further development of it has been expected.

In recent years, Autonomous Emergency Braking System (AEBS) has been drawing attention as a technology to reduce the number of traffic accidents. The outline of AEBS is as follows: when a camera or a radar mounted in a vehicle detects an obstacle such as another vehicle or a pedestrian in front, the danger of collision is judged from the relative position and the relative speed, and the system decelerates the vehicle. According to the survey of a vehicle manufacturer, the total number of accidents has decreased by 61% compared with non-equipped vehicles, and the number of rear-end accidents has decreased by 84% [(4)]. It proves the importance and the usefulness of AEBS.

However, current AEBS in commercial vehicles detects the danger of collision based on the current position of a pedestrian, and there is a problem that it does not consider the pedestrian movement. In case of a pedestrian or an obstacle exists in front of the vehicle, the system can deal with it, and it is possible to avoid the collision accident. On the other hand, when a pedestrian walks from the side, the current AEBS may not work because the pedestrian is not positioned in front of the vehicle until the moment of collision. Since collision accidents between a pedestrian and a vehicle often happen while crossing the road, AEBS corresponding to the pedestrian movement is an important system for reducing traffic accidents.

Corresponding to a pedestrian movement, it is necessary to predict a pedestrian's future position and control the braking force accordingly. Therefore, it is necessary to control the vehicle in the time domain such that the position of the vehicle in the finite time is the command value of the system.

Then, Model Predictive Control (MPC) has attracted attention as a controller design method in the time domain. MPC can be called a real-time optimal control with constraints, which predicts the system behavior to the future, and determines the current input value so as to minimize the evaluation function [(5)]. MPC needs to solve quadratic programming problems and has been widely used the system with the long sampling time such as a field of process control because of large calculation load. However, the calculation speed of computers has improved in recent years, which makes it possible to apply to systems with the short sampling time. As another problem of MPC, it is an open-loop controller. Control performance largely depends on the model accuracy and it has a disadvantage that the sensitivity of the disturbance is high.

In order to satisfy both of the disturbance suppression and the followability to a target value, it is necessary to estimate disturbance and compensate by feedforward control. Disturbance refers to the driving resistance such as the rolling resistance, the air resistance, and gradient resistance generated when running on a slope. However, most of the previous studies of driving force control ignore the assumption that the driving resistance is very small [(6)]. In the case of a system with a short sampling time, it is possible to reduce the influence of the driving resistance by the feedback loop. However,

a) Correspondence to: Yusuke Nakamura. E-mail: nakamura@sum.sd.keio.ac.jp
* Keio University
3-14-1, Hiyoshi, Kohoku-ku, Yokohama, Kanagawa 223-8522, Japan

MPC has a longer sampling time than the PID control and the like, and the influence of the disturbance becomes conspicuous. Furthermore, the disturbance reduces the accuracy of the model used for prediction in MPC, so that the predicted behavior of the automobile deviates from the actual one. It leads to failure to obtain a desired result. Therefore, to apply MPC to the driving force control, it is necessary to consider estimating and compensating the driving resistance.

Generally, human drives while making danger prediction based on various road environments and pedestrians. Here, this research aims to control the vehicle while predicting the danger such as human, and it leads to improve AEBS to correspond to the pedestrian movement. In order to achieve this purpose, it is mentioned about building an algorithm to predict the pedestrian's future position and designing controllers in the time domain which can compensate for the driving resistance.

This paper assumes that the position information of a pedestrian obtained from a sensing device such as a camera mounted on the vehicle. The outline of the proposed method is as follows. First, the pedestrian velocity is estimated from the current pedestrian's position by Kalman filter. The pedestrian's forecast position in the future is predicted from the values of the pedestrian velocity for a certain period of time. If there is a possibility of the collision, the command value of the braking force is calculated by MPC as compared with the predicted position of the vehicle. Since MPC depends on the model accuracy, it has a disadvantage that it is strongly affected by the disturbance and the parameter error. Therefore, a feedback loop of the braking force is introduced so as to improve the control performance, and the estimator of driving resistance which is a disturbance is included to the proposed system. The controller of the system is a cascade controller of MPC and braking force feedback control. By utilizing the proposed method, it is possible to predict the pedestrian's position of the future and to detect the danger of collision. Furthermore, compensating the driving resistance and controlling the braking force, it is possible to improve the followability of the system while reducing the disturbance sensitivity.

This paper is organized as follows. In Section 2, the modeling used in the proposed method is explained, and the design of the control system is discussed in Section 3. In sections 4 and 5, the simulation and the experiment is explained, respectively. Finally, the conclusion is shown in Section 6.

2. Modeling

2.1 Chassis Model The collision among the vehicle and a pedestrian is almost happened on a straight road, and in order to simplify model, the vehicle's chassis model only considering linear movement is shown in Fig. 1.

As shown in Fig. 1, the kinematics and dynamics of the vehicle's chassis is as follows:

$$\dot{x} = v\cos\theta, \quad \cdots\cdots (1)$$

$$\dot{y} = v\sin\theta, \quad \cdots\cdots (2)$$

$$M\dot{v} = nF_d + F_r, \quad \cdots\cdots (3)$$

where x and y are the position of the vehicle. v, θ, M, n, F_d, and F_r denote the vehicle velocity, the vehicle angle, the vehicle mass, the number of controlled wheels, the driving force, and the driving resistance, respectively. ΣW denotes the world coordinate system. Therefore, x and y in ΣW indicate the position of latitude and longitude, respectively. In general, the resistance force faces in the opposite direction against the one of travel. However, the driving resistance can be positive and also negative, and F_r faces in the same direction of F_d in this paper.

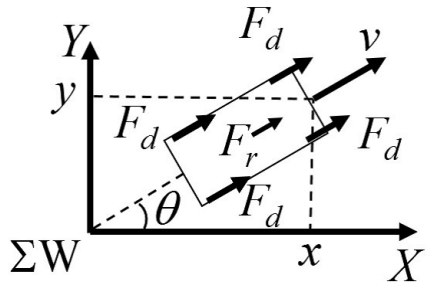

Fig. 1. The vehicle's chassis model

Incidentally, the control method of this paper includes Model Predictive Control (MPC), and MPC is formulated in discrete-state. Therefore, the discrete-time state space representation of the chassis model confined only linear movement is expressed as follows:

$$\boldsymbol{x}[k+1] = \boldsymbol{A}\boldsymbol{x}[k] + \boldsymbol{B}(u[k] + F_r), \quad \cdots\cdots (4)$$

$$z[k] = \boldsymbol{C}\boldsymbol{x}[k], \quad \cdots\cdots (5)$$

with

$$\boldsymbol{A} = \begin{bmatrix} 1 & 0 & T_s\cos\theta \\ 0 & 1 & T_s\sin\theta \\ 0 & 0 & 1 \end{bmatrix},$$

$$\boldsymbol{B} = \begin{bmatrix} \frac{1}{2M}T_s^2\cos\theta & \frac{1}{2M}T_s^2\sin\theta & \frac{T_s}{M} \end{bmatrix}^T,$$

$$\boldsymbol{C} = \boldsymbol{I_3},$$

$$u[k] = nF_d,$$

$$\boldsymbol{x}[k] = \begin{bmatrix} x & y & v \end{bmatrix}^T,$$

where T_s denotes the sampling time. $u[k]$ is the sum of the tire force of each wheel, and the output variables of the system equals the state variables. It indicates that the system can acquire the information about x, y, and v. Since the position of the vehicle can be measured with high accuracy due to the development of positioning technology such as Quasi-Zenith Satellite System (QZSS) in Japan, this paper assumes that these values can be acquired [7].

2.2 Wheel Model The dynamics of the wheel model as shown in Fig. 2 is described as follows:

$$J\dot{\omega} = T_m - r_w F_d, \quad \cdots\cdots (6)$$

$$F_d = \mu(\lambda)\frac{Mg}{n}, \quad \cdots\cdots (7)$$

$$\lambda = \frac{v - r_w\omega}{\max(v, r_w\omega)}, \quad \cdots\cdots (8)$$

where J, T_m, ω, r_w, λ, and μ denote the motor inertia, the torque generated by a motor or a braking device, the wheel angular velocity, the wheel radius, the slip ratio, and the friction coefficient, respectively. It is note that μ is a function of slip ratio λ, and μ denotes the ratio of the normal force and the tire force.

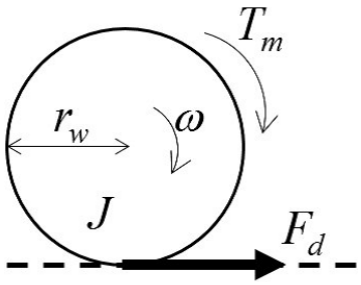

Fig. 2. The vehicle's wheel model

2.3 Friction Circle According to the friction circle theory, the tire force including the longitudinal force F^x and the lateral force F^y must be satisfied with Eq. (9) [8].

$$\sqrt{F^{x2} + F^{y2}} \leq \mu_{max} Mg \cdots\cdots\cdots\cdots\cdots\cdots\cdots (9)$$

μ_{max} indicates the maximum friction coefficient, and g is the gravitational acceleration. Equation (9) shows that the resultant force of the longitudinal force and lateral force has an upper limit. In the case of that the resultant force exceeds the right side of Eq. (9), the tire is going to slip, and a driver cannot control the vehicle. Therefore, it is necessary to control the tire force to avoid the slip phenomenon.

3. Control System Design

This section explains the proposed control system, which is constructed from 2 sections [9]. one is the part of collision detection and the other one is the braking system.

3.1 Collision Detection In order to detect the collision among a pedestrian and a vehicle, the pedestrian's velocity is estimated using Kalman filter at first. The state-space representation and the estimate equation are described as follows:

$$\boldsymbol{x_h}[k+1] = \boldsymbol{A_k}\boldsymbol{x_h}[k] + \boldsymbol{G_k}\boldsymbol{\omega}, \cdots\cdots\cdots\cdots\cdots (10)$$

$$\boldsymbol{z_h}[k] = \boldsymbol{c_k}\boldsymbol{x_h}[k] + \boldsymbol{J_k}\boldsymbol{\nu}, \cdots\cdots\cdots\cdots\cdots\cdots (11)$$

$$\hat{\boldsymbol{x_h}}[k] = \boldsymbol{A_k}\hat{\boldsymbol{x_h}}[k-1] + \boldsymbol{g}[k](\boldsymbol{z_h}[k] - \boldsymbol{c_k}\boldsymbol{A_k}\hat{\boldsymbol{x}}_h[k-1]), \cdots\cdots\cdots (12)$$

with

$$\boldsymbol{A_k} = \begin{bmatrix} 1 & 0 & T_s & 0 \\ 0 & 1 & 0 & T_s \\ 0 & 0 & 1 & 0 \\ 0 & 0 & 0 & 1 \end{bmatrix},$$

$$\boldsymbol{G_k} = \begin{bmatrix} \frac{1}{2}T_s^2 & 0 & T_s & 0 \\ 0 & \frac{1}{2}T_s^2 & 0 & T_s \end{bmatrix}^T,$$

$$\boldsymbol{c_k} = \begin{bmatrix} 1 & 0 & 0 & 0 \\ 0 & 1 & 0 & 0 \end{bmatrix},$$

$$\boldsymbol{J_k} = \boldsymbol{I_2},$$

$$\boldsymbol{x_h}[k] = \begin{bmatrix} x_h[k] & y_h[k] & \dot{x_h}[k] & \dot{y_h}[k] \end{bmatrix}^T,$$

$$\boldsymbol{z_h}[k] = \begin{bmatrix} x_h[k] & y_h[k] \end{bmatrix}^T,$$

where $\boldsymbol{\omega}$, $\boldsymbol{\nu}$, and $\boldsymbol{g}[\boldsymbol{k}]$ denote the system noise, the observation noise, and the optimal kalman gain, respectively. It is note that $\boldsymbol{\omega}$ and $\boldsymbol{\nu}$ are the white noise. x_h and y_h are the position of a pedestrian which are obtained by the camera device or the road equipment. Utilizing Kalman filter, it is possible to estimate the pedestrian's velocity.

Table 1. Relationship among f and c [10]

f	c
0.393	1.000
0.500	1.177
0.900	2.146
0.950	2.448
0.990	3.035

Next, the pedestrian's position in the finite time is predicted from the pedestrian's velocity. It is assumed that a pedestrian's velocity in a definite period of time follows the quadratic normal distribution, which makes the equal probability ellipse if the probability destiny function is constant. The equation of the equal probability ellipse is shown as follows:

$$\frac{\left((x-\mu_x)\cos\alpha + \left(y-\mu_y\right)\sin\alpha\right)^2}{(c\sigma_u)^2} + \frac{\left(-(x-\mu_x)\cos\alpha + \left(y-\mu_y\right)\sin\alpha\right)^2}{(c\sigma_v)^2} = 1, \cdots (13)$$

with

$$\sigma_u^2 = \frac{\sigma_x^2 + \sigma_y^2 + \sqrt{\left(\sigma_x^2 - \sigma_y^2\right) + 4\sigma_{xy}^2}}{2},$$

$$\sigma_v^2 = \frac{\sigma_x^2 + \sigma_y^2 - \sqrt{\left(\sigma_x^2 - \sigma_y^2\right) + 4\sigma_{xy}^2}}{2},$$

$$\alpha = \arctan\frac{\sigma_u^2 - \sigma_x^2}{\sigma_{xy}},$$

where μ_x and μ_y are the mean value, and σ_x, σ_y are the standard deviation, and σ_{xy} is the covariance of the pedestrian's velocity. Additionally, α denotes the angle of the equal probability ellipse. c depends on the probability destiny function f, and the relationship between c and f is shown in Table 1 [10]. Therefore, Eq. (13) indicates the pedestrian's forecast position in 1 second. On the other hand, the vehicle's forecast position without the input is formulated as follows:

$$\hat{\boldsymbol{x}}[k+i|k] = \boldsymbol{A}^i\hat{\boldsymbol{x}}[k|k] + \boldsymbol{B}F_r, \cdots\cdots\cdots\cdots\cdots (14)$$

$i = 1, 2, ..., H_p$, and H_p is a prediction horizon. Next, it is mentioned about the collision detection. It can be confirmed whether there is a possibility of the collision between a vehicle and a pedestrian by calculating following equations.

$$D = \frac{(a+b)^2}{(c\sigma_u(iT_s+\tau)+R_h)^2} + \frac{(-a+b)^2}{(c\sigma_v(iT_s+\tau)+R_h)^2} \cdots\cdots\cdots\cdots\cdots (15)$$

$$a = (\hat{x}_1[k+i|k] - \mu_x(iT_s+\tau) - x_h)\cos\alpha$$

$$b = \left(\hat{x}_2[k+i|k] - \mu_y(iT_s+\tau) - y_h\right)\sin\alpha$$

R_h and τ denote a radius of the safety zone for a pedestrian and the calculation dead time, respectively. x_h and y_h are the current position of the pedestrian, and μ_x, and μ_y are the mean of the pedestrian's velocity within a certain period of time. If D is less than 1, it is necessary to decelerate to avoid

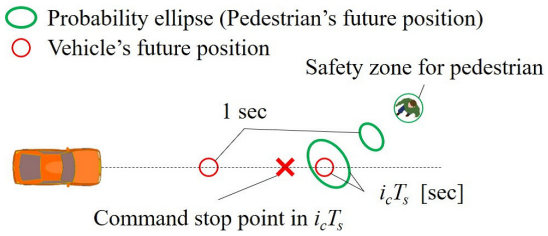

Fig. 3. The outline figure of collision detection

the collision because the vehicle would be in the pedestrian's forecast position. The command for the vehicle stop position is determined by solving simultaneous equations for x and y as follows:

$$\begin{cases} \dfrac{(a'+b')^2}{(c\sigma_u(i_cT_s+\tau)+R_h)^2}+\dfrac{(-a'+b')^2}{(c\sigma_v(i_cT_s+\tau)+R_h)^2}=1 \\ y=\boldsymbol{x}_3[k|k]\tan\theta x-\boldsymbol{x}_1[k|k]\boldsymbol{x}_3[k|k]\tan\theta+\boldsymbol{x}_2[k|k] \end{cases}, \cdots\cdots\cdots\cdots\cdots (16)$$

$$a' = (x-\mu_x(i_cT_s+\tau)-x_h)\cos\alpha,$$
$$b' = \left(y-\mu_y(i_cT_s+\tau)-y_h\right)\sin\alpha.$$

i_c is the smallest i that satisfies $D \leq 1$ in Eq. (15). The solution which is nearer to the vehicle's current position is adopted as the limit stop position of the collision avoidance, and the command stop point in i_cT_s is the position at a fixed distance from the limit position. Figure 3 shows the outline of the process of the collision detection.

3.2 Control of Braking System Model Predictive Control (MPC) is used to decelerate the vehicle to stop at the command stop point in i_cT_s. MPC is a control method that optimizes the input while predicting the future response at each time with some constraints [5]. The evaluation function is as follows:

$$V[k] = \|\boldsymbol{Z}[k]-\boldsymbol{T}[k]\|_Q^2+\|\Delta\boldsymbol{U}[k]\|_R^2, \cdots\cdots\cdots (17)$$

with

$$\boldsymbol{Z}[k]=\begin{bmatrix} z[k+H_w|k] \\ \vdots \\ z\left[k+H_p|k\right] \end{bmatrix},$$
$$\boldsymbol{T}[k]=\begin{bmatrix} r[k+H_w|k] \\ \vdots \\ r\left[k+H_p|k\right] \end{bmatrix},$$
$$\boldsymbol{\Delta U}(k)=\begin{bmatrix} \Delta\hat{u}(k|k) \\ \vdots \\ \Delta\hat{u}(k+H_u-1|k) \end{bmatrix},$$

where H_u is control horizon. $\boldsymbol{Q}$ and $\boldsymbol{R}$ are described as follows:

$$\boldsymbol{Q}=\begin{pmatrix} \boldsymbol{Q}(H_w) & 0 & \cdots & 0 \\ 0 & \boldsymbol{Q}(H_w+1) & \cdots & 0 \\ \vdots & \vdots & \ddots & \vdots \\ 0 & 0 & \cdots & \boldsymbol{Q}\left(H_p\right) \end{pmatrix},$$

$$\boldsymbol{R}=\begin{pmatrix} \boldsymbol{R}(0) & 0 & \cdots & 0 \\ 0 & \boldsymbol{R}(1) & \cdots & 0 \\ \vdots & \vdots & \ddots & \vdots \\ 0 & 0 & \cdots & \boldsymbol{R}(H_u-1) \end{pmatrix},$$

where H_w is a window parameter which indicates the input dead time. $\boldsymbol{Q}$ and $\boldsymbol{R}$ denote the weight matrices of the output error and the input change, respectively. The first term on the right-hand side in Eq. (17) has the effect of reducing the error from the command value, and the second term suppresses a sudden change of the input. $\boldsymbol{r}[k+i]$ is determined as follows:

$$\boldsymbol{r}[k+i]^T=\begin{pmatrix} x_s & y_s & 0 \end{pmatrix} \quad i_c \leq i \leq H_p \cdots\cdots (18)$$

Equation (18) indicates the vehicle position in i_cT_s [sec] and later. Incidentally, the constraints of the output and the input change and the input is as follows:

$$|\hat{z}_1[k+i|k]-z_1[k|k]| \leq |x_s-z_1[k|k]|, \cdots\cdots\cdots (19)$$
$$|\hat{z}_2[k+i|k]-z_2[k|k]| \leq |y_s-z_2[k|k]|, \cdots\cdots\cdots (20)$$
$$|\Delta\hat{u}[k+i|k]| \leq \Delta u_{max}, \cdots\cdots\cdots\cdots\cdots\cdots (21)$$
$$-\hat{\mu}_{\max}Mg \leq u[k+i|k] \leq 0. \cdots\cdots\cdots\cdots\cdots\cdots (22)$$

Equations (19)–(20) are the role for not running past the command stop point, and Eq. (21) indicates the input change is less than Δu_{max} which is the tuning parameter. Equation (22) makes the tire force smaller than the maximum braking force determined by the friction circle theory. Minimizing Eq. (17) under constraints shown in Eqs. (19)–(22), the optimal input change $\Delta u[k|k]$ is calculated. Therefore, the optimal braking force of each wheel is determined as follows:

$$F_d^{cmd} = u[k-1]+\Delta u[k|k]. \cdots\cdots\cdots\cdots\cdots\cdots (23)$$

So MPC is an open-loop controller that a feedback loop is necessary to compensate the modeling error. Hence, it is proposed to provide the feedback loop of the tire force inside of MPC. Therefore, the reference torque generated by the braking device is determined as follows:

$$T_m^{ref} = \frac{K_i}{s}\left(F_d^{cmd}-\hat{F}_d\right), \cdots\cdots\cdots\cdots\cdots\cdots (24)$$

where K_i, and $\hat{F}_d$ denote the integral gain, and the estimated value of the tire force by Driving Force Observer (DFOB), respectively.

3.3 Observer Design In this section, it is mentioned about the method to estimate the tire force and the driving resistance. In order to estimate the tire force, Driving Force Observer (DFOB) is utilized [12]. DFOB is based on Disturbance Observer (DOB), which can estimate disturbance torque accurately [11]. DFOB is formulated as follows:

$$\hat{F}_d = \frac{1}{r_w}\left(\frac{g_{cut}}{s+g_{cut}}\left(T_m^{ref}+g_{cut}J\omega\right)-g_{cut}J\omega\right), \cdots (25)$$

where g_{cut} denotes the cut-off frequency of Low-Pass Filter(LPF). The block diagram of DFOB is shown in Fig. 4. It is necessary to estimate the driving resistance F_r for enhancing the control performance, and it can be estimated by using Eq. (26). The block diagram of the driving resistance estimator is shown in Fig. 5.

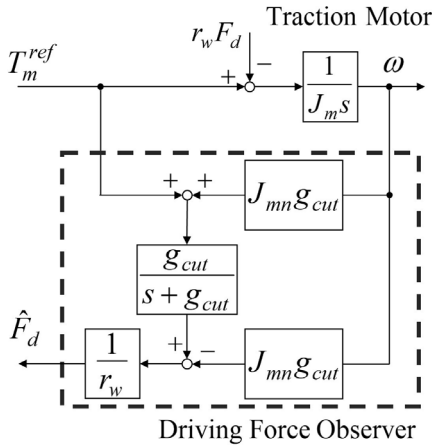

Fig. 4. Block diagram of DFOB

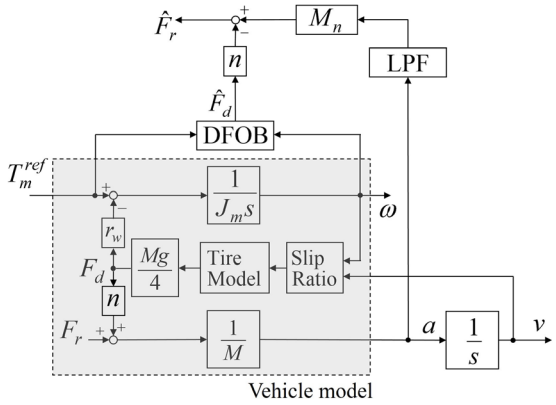

Fig. 5. Block diagram of driving resistance estimation

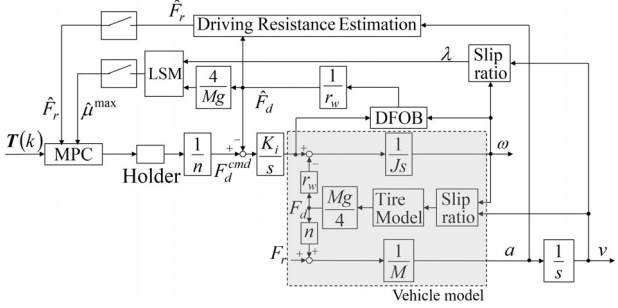

Fig. 6. Block diagram of whole brake system

$$\hat{F}_r = M\frac{g_{cut}}{s+g_{cut}}a - n\hat{F}_d \quad \cdots\cdots (26)$$

a is the vehicle's longitudinal acceleration.

μ can be estimated by Eq. (7), and λ is calculated by Eq. (8). Acquiring λ and μ successively, the maximum friction coefficient μ_{max} is estimated by approximating μ–λ curve to the quadratic function using Least Square Method (LSM) and set μ_{max} as the constraint of MPC in Eq. (22).

Finally, the entire of braking system is shown in Fig. 6.

4. Simulation

4.1 Simulation Condition To verify the effectiveness of the proposed method, the simulation has been carried out. The scenario was that a pedestrian came out from side, and stopped when arriving in front of the vehicle as shown in Fig. 7. N represents the normal distribution,

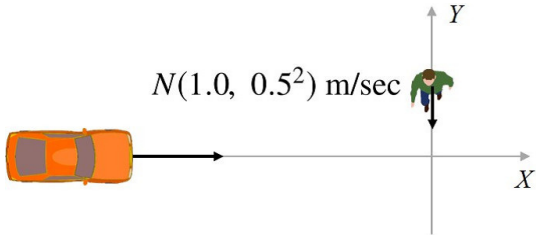

Fig. 7. Situation of simulation

Table 2. The road environment in the simulation

Road	Surface	Gradient
1	Dry	Downhill
2	Wet	Flat

Table 3. The simulation condition

Parameter	Value	Unit
Vehicle mass M	1000	kg
Wheel radius r_w	0.302	m
Number of controlled wheels n	4	–
Motor Inertia J_{wh}	1.24	kgm^2
Motor viscosity coefficient D_{wh}	0.00040	Nsec/m
Motor coulomb friction f_{wh}	0.001	N
Sample time in MPC T_s	0.1	sec
Integral gain K_i	50000	–
prediction horizon H_p	30	–
Control horizon H_u	10	–
Safety zone for pedestrian R_h	0.5	m
Downhill gradient θ_p	5	deg
Rolling resistance coefficient C_{rr}	0.01	–
Air resistance coefficient C_d	0.3	–
Projected area S	1.754	m^2
Air density ρ	1.225	kg/m^3

therefore a pedestrian walked at the velocity of the average is 1.0 m/sec and the standard deviation is 0.5 m/sec. The simulation was carried out at 2 kinds of the road environment, which is shown in Table 2.

Reproducing the road surface, Magic Formula tire model was utilized in this simulation [13]. The driving resistance consists of the rolling resistance, the air resistance and the gradient resistance. Each force is formulated in Eqs. (27)–(30).

$$F_{roll} = -C_{rr}Mg \quad \cdots\cdots (27)$$

$$F_{air} = -\frac{1}{2}\rho C_D S v^2 \quad \cdots\cdots (28)$$

$$F_{grad} = Mg\sin\theta_{grad} \quad \cdots\cdots (29)$$

$$F_r = F_{roll} + F_{air} + F_{grad} \quad \cdots\cdots (30)$$

The simulation parameters are shown in Table 3. In simulation 1, the comparison is made on whether driving resistance is compensated when driving at the road environment 1. Additionally, the comparison is made on the presence or absence of the maximum friction coefficient estimation at the road environment 2.

4.2 Simulation Results The results of the simulation 1 are shown in Figs. 8–10. Figure 8 indicates the position of the vehicle and a pedestrian. According to Fig. 8, the system performed well so that the vehicle stopped forward a pedestrian by compensating the driving resistance. In case of absence of the driving resistance compensation, the vehicle couldn't stop in front of a pedestrian. Therefore, it is verified to compensate the driving resistance.

In addition, Fig. 9 shows the comparison of the estimated

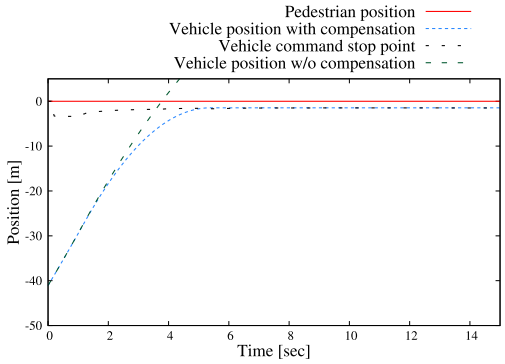

Fig. 8. Simulation 1 result of vehicle position

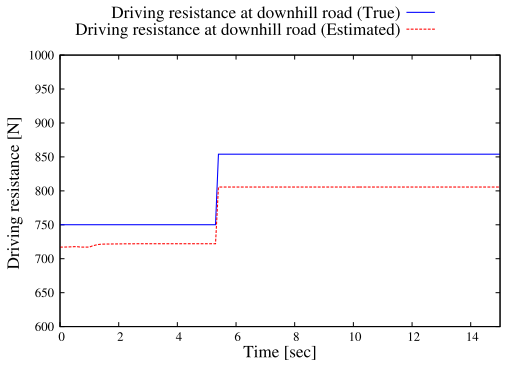

Fig. 9. Simulation 1 result of driving resistance

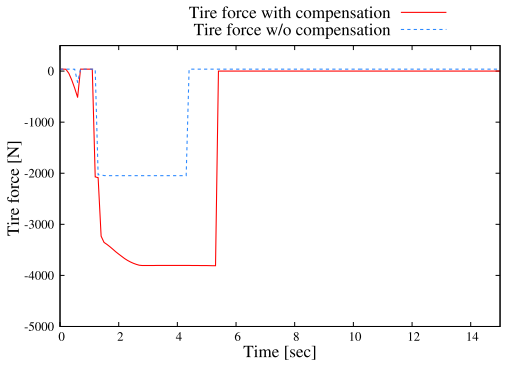

Fig. 10. Simulation 1 result of tire force

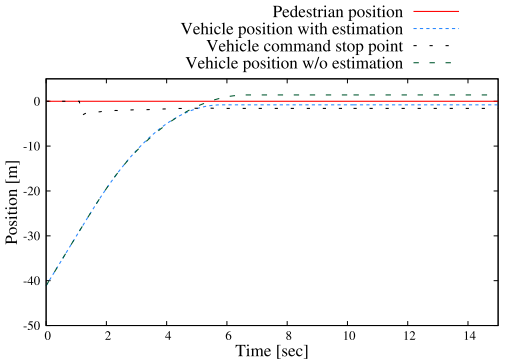

Fig. 11. Simulation 2 result of vehicle position

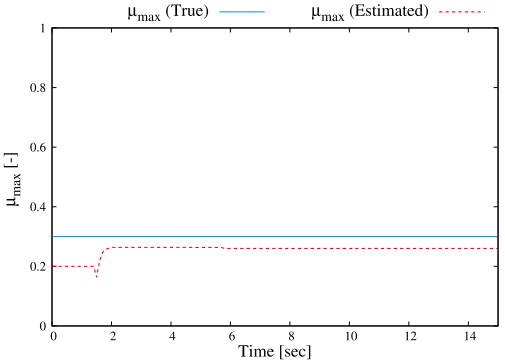

Fig. 12. Simulation 2 result of maximum friction coefficient

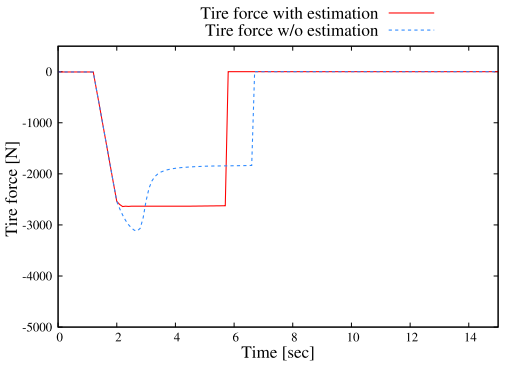

Fig. 13. Simulation 2 result of tire force

value and the true value of the driving resistance, and it indicates that the value was closed to the true value. It is confirmed that the appropriate braking force is generated in the proposed method from Fig. 10. In case of utilizing the control method with compensation, the braking force considering the driving force is added to the vehicle. Road environment 1 is a downhill road, and the driving resistance includes the positive gradient resistance. Hence, it is necessary to brake the vehicle strongly to stop the command point. Similarly, the results of the simulation 2 are shown in Figs. 11–13.

Figure 11 indicates positions of the vehicle and a pedestrian. According to Fig. 11, the vehicle stopped forward a pedestrian by estimating the maximum friction coefficient even the road surface is wet. Figure 12 shows the result of the maximum friction coefficient estimation, and it indicates that the estimate value converged to a value which is slightly smaller than true one. It is confirmed that the appropriate braking force is generated in the proposed method from Fig. 10. In case of not estimating the maximum friction coefficient, the absolute value of the tire force decreased from 2.4 sec. It indicates that braking force exceeds the limitation in the friction circle theory, and the tire became slip. Therefore, the effectiveness was confirmed to the estimate maximum friction coefficient.

5. Experiment

The experiment had been carried out in order to ensure the effectiveness of the proposed method. In the experiment, RoboCar 1/10 which is a 1:10 scale vehicle model produced by ZMP Inc. was used as shown in Fig. 14. This model includes the speed controller, and the input of the system is only the velocity of the vehicle. Therefore, the velocity value obtained from MPC is utilized for the input, and the vehicle velocity feedback was implemented instead of the driving force feedback. The block diagram in the experiment is shown in Fig. 15. Table 4 shows the experimental setup, and

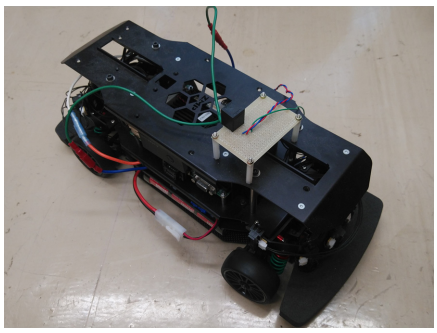

Fig. 14. Experimental vehicle

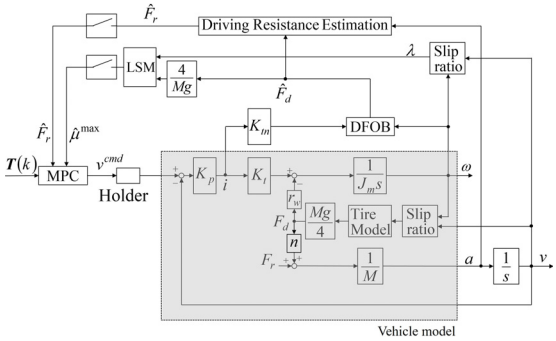

Fig. 15. Block diagram in experiment

Table 4. Experimental parameters

Parameter	Value	Unit
Vehicle mass M	2.9	kg
Number of controlled wheels n	2	–
Sample time in MPC T_s	0.1	sec
Proportional gain K_p	50	–
prediction horizon H_p	30	–
Control horizon H_u	10	–
Safety zone of pedestrian R_h	0.05	m
Torque coefficient K_t	0.002354	–
Motor inertia J_m	4.342×10^{-6}	kgm^2
Motor viscosity coefficient D_{wh}	9.416×10^{-7}	Nmsec/rad
Motor coulomb friction f_{wh}	2.532×10^{-3}	Nm

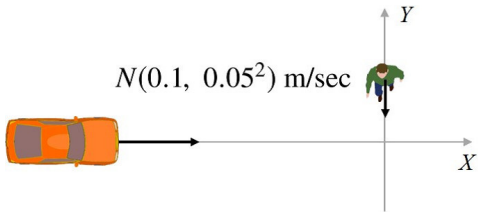

Fig. 16. Situation of experiment

the experimental procedure is as follows.

- step1 : PC generates the virtual pedestrian's position
- step2 : PC sends the information to the vehicle
- step3 : The vehicle receives the pedestrian's position and carries out the control

The position of a pedestrian was calculated by PC following Fig. 16.

The experimental results are shown in Figs. 17, 18. Figure 17 shows the position of the vehicle and a pedestrian. The vehicle stopped at near the command stop point in front of a pedestrian. It indicated that the proposed method performs very well as the collision avoidance system. According to Fig. 18, the driving resistance estimator converges to the

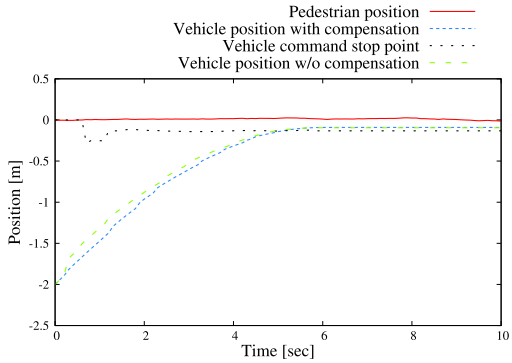

Fig. 17. Experimental result of vehicle position

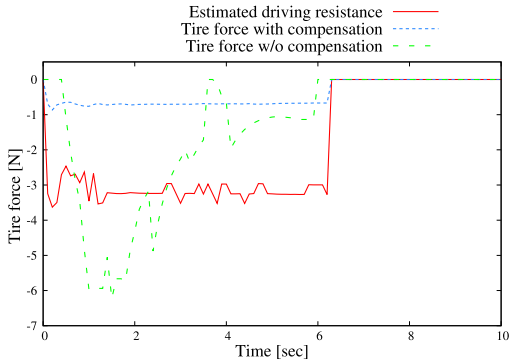

Fig. 18. Experimental result of tire force

steady-state value. However, compared with the simulation results, the driving resistance was much larger than the driving force. This phenomenon was caused by the tire which has a large rolling resistance, therefore the braking force should be controlled appropriately to stop the vehicle at the command stop point. In case of the braking system without the compensation, the braking force was fluctuated. The reason why is that the driving resistance affected the system as the disturbance and MPC could not predict the vehicle state accurately. From the above, the effectiveness of the proposed method was confirmed through the experiment.

6. Conclusion

The purpose of this paper is to realize the automated deceleration system to avoid the collision with a pedestrian. The proposed system can predict the pedestrian's future position from the current position, and detect the collision probability. Furthermore, the controller with MPC which can compensate the driving resistance and the modeling error is also proposed in this paper.

The outline of the proposed method is as follows. First, the pedestrian velocity is estimated from the current pedestrian's position by Kalman filter. The pedestrian's forecast position in the future is predicted from the pedestrian velocity, and the command value of the braking force is calculated by MPC. Here, since MPC is strongly affected by the disturbance and the parameter error, a feedback loop of braking force is proposed so as to improve the control performance. In addition, the estimator of driving resistance is included to the proposed system. By utilizing the proposed method, it is possible to predict the pedestrian's position of the future and to detect the danger of the collision. Furthermore,

compensating the driving resistance and controlling the braking force, it is possible to improve the followability of the system while reducing the disturbance sensitivity.

The effectiveness of the proposed method is verified through the simulation and the experiment. Utilizing this system, it is expected to reduce the number of accidents.

References

(1) Z. Wei and G. Xuexun: "An ABS Control Strategy for Commercial Vehicle", *IEEE/ASME Transactions on Mechatronics*, Vol.20, No.1, pp.384–392 (2015)

(2) S. Sakai, H. Sado, and Y. Hori: "Motion Control in an Electric Vehicle with Four Independently Driven In-Wheel Motors", *IEEE/ASME Transactions on Mechatronics*, Vol.4, No.1, pp.9–15 (1999)

(3) T. Takano, H. Nobumoto, T. Okazaki, and H. Fujimoto: "Driving Force Control Method Based on High Accuracy Slip Ratio Control", *Mazda Technical Review*, No.32, pp.228–233 (2015)

(4) S. Usui, N. Nomrua, H. Kumagai, and H. Sekine: "Development og Improvements to Driver Assistence System "EyeSight" for Reduction of Traffic Accidents", *Journal of the Japan Society of Applied Electromagnetics and Mechanics*, Vol.25, No.4, pp.383–389 (2017)

(5) J.M. Maciejowski, S. Adachi, and M. Kannno: "Predictive Control with Constraints", Tokyo Denki University Press (2005)

(6) J. Guo, P. Hu, and R. Wang: "Nonlinear Coordinated Steering and Braking Control of Vision-Based Autonomous Vehicles in Emergency Obstacle Avoidance", *IEEE Transactions on Intelligenttransportationsystems*, Vol.17, No.11, pp.3230–3240 (2016)

(7) H. Namie, O. Okamoto, N. Kubo, and A. Yasuda: "Initial Performance Evaluation of cm-class Augmentation System using Quasi-Zenith Satellite System", *IEEJ Transactions on Industry Aoolications*, Vol.138, No.3, pp.173–179 (2018)

(8) E. Ono, Y. Hattori, and Y. Muragishi: "Estimation of Tire Frinction Circle and Vehicle Dynamics Integrated Control for Four-wheel Distributed Steering and Four-wheel Distributed Traction/Braking Systems", *R&D Review of Toyota CRDL*, Vol.40, No.4, pp.7–13 (2005)

(9) Y. Nakamura, T. Nozaki, and T. Murakami: "Automated Deceleration System Considering Driving Resistance Based on Pedestrian's Forecast Position", *The IEEJ International Workshop on Sensing, Actuaion, Motion Control, and Optimization* (2018)

(10) K. Komaki and M. Tajima: "Saishojijoho to Sokuryomo Heikin no Kiso", Toyo Shoten (2001)

(11) K. Ohnishi: "Robust Motion Control by Disturbance Observer", *Journal of the Robotics Society of Japan*, Vol.11, No.4, pp.486–493 (1993)

(12) H. Sado, S. Sakai, and Y. Hori: "Road Condition Estimation for Traction Control in Electric Vehicle", *IEEE Proc. on Industrial Electronics*, Vol.2, pp.973–978 (1999)

(13) H.B. Pacejka and E. Bakker: "The Magic Formula Tyre Model", *Vehicle System Dynamics*, Vol.21, pp.1–18 (1993)

Yusuke Nakamura (Student Member) received the B.E. degrees from Keio University, Yokohama, Japan, in 2018. He is currently graduate student in Keio University.

Toshiyuki Murakami (Fellow) received the B.E., M.E., and Ph.D. degrees in electrical engineering from Keio University, Yokohama, Japan, in 1988, 1990, and 1993, respectively. In 1993, he joined the Department of Electrical Engineering, Keio University, where he is currently a Professor in the Department of System Design Engineering. From 1999 to 2000, he was a Visiting Researcher with The Institute for Power Electronics and Electrical Drives, Aachen University of Technology, Aachen, Germany.